Structure and Ligand Binding Determinants of the Recombinant Kringle 5 Domain of Human Plasminogen[†,‡]

Yuan Chang,[§] Igor Mochalkin,[∥] Stephen G. McCance,[§] Beisong Cheng,[∥] Alexander Tulinsky,*[,∥] and Francis J. Castellino*[,§]

Department of Chemistry and Biochemistry, University of Notre Dame, Notre Dame, Indiana 46556, and Department of Chemistry, Michigan State University, East Lansing, Michigan 48824

Received September 15, 1997; Revised Manuscript Received December 9, 1997

ABSTRACT: The X-ray crystal structure of the recombinant (r) kringle 5 domain of human plasminogen ($K5_{HPg}$) has been solved by molecular replacement methods using $K1_{HPg}$ as a model and refined at 1.7 Å resolution to an *R* factor of 16.6%. The asymmetric unit of $K5_{HPg}$ is composed of two molecules related by a noncrystallographic 2-fold rotation axis approximately parallel to the *z*-direction. The lysine binding site (LBS) is defined by the regions His^{33}-Thr^{37}, Pro^{54}-Val^{58}, Pro^{61}-Tyr^{64}, and Leu^{71}-Tyr^{74} and is occupied in the apo-form by water molecules. A unique feature of the LBS of apo-$K5_{HPg}$ is the substitution by Leu^{71} for the basic amino acid, arginine, that in other kringle polypeptides forms the donor cationic center for the carboxylate group of ω-amino acid ligands. While wild-type (wt) r-$K5_{HPg}$ interacted weakly with these types of ligands, replacement by site-directed mutagenesis of Leu^{71} by arginine led to substantially increased affinity of the ligands for the LBS of $K5_{HPg}$. As a result, binding of ω-amino acids to this mutant kringle (r-$K5_{HPg}[L^{71}R]$) was restored to levels displayed by the companion much stronger affinity HPg kringles, $K1_{HPg}$ and $K4_{HPg}$. Correspondingly, alkylamine binding to r-$K5_{HPg}[L^{71}R]$ was considerably attenuated from that shown by wtr-$K5_{HPg}$. Thus, employing a rational design strategy based on the crystal structure of $K5_{HPg}$, successful remodeling of the LBS has been accomplished, and has resulted in the conversion of a weak ligand binding kringle to one that possesses an affinity for ω-amino acids that is similar to $K1_{HPg}$ and $K4_{HPg}$.

Kringles are modular units present in a variety of functionally distinct proteins, among which are those involved in blood coagulation and fibrinolysis. The prototypical kringle domain consists of approximately 80 amino acids arranged in a rigidly conserved triple disulfide bond pattern of 1−6, 2−4, and 3−5. Multiple copies of these motifs can exist in proteins. In a striking example of this, a range encompassing 12−41 kringles has been found in alleles of Lp(a)[1] *(1, 2)*, and the number of kringle units in this protein has been correlated to increased risk of coronary heart disease *(3)*. With regard to the human-derived proteins involved in fibrinolysis, one kringle module exists in uPA *(4)*, tPA possesses two such structural units *(5)*, and HPg contains five kringle motifs *(6)*. The kringles of HPg and HPm serve as functional-binding loci for other plasma proteins *(7−11)*, for the fibrin clot *(8, 12)*, for a variety of cell types *(13−15)*, and for cell-associated proteins *(16, 17)*.

Many of the kringle-dependent interactions of HPg and HPm are inhibited by ω-amino acids that occupy the LBS of the kringle, such as the widely studied model ligand, EACA. Correspondingly, the binding of HPg and HPm to certain proteins, such as α_2-antiplasmin *(10, 18)* and enolase *(19)*, is enhanced by the presence of C-terminal lysine residues in these proteins. A specific functional example of the importance of the LBS of HPg and HPm kringles is the finding that the HPm-catalyzed digestion of native fibrin clots, a process that exposes C-terminal lysine residues of fibrin, enhances binding of HPg and HPm to the degrading fibrin and by this mechanism stimulates clot lysis *(20, 21)*. In an extension of these findings, it has been demonstrated that release from the protein of these fibrin C-terminal lysine residues by catalysis via a plasma carboxypeptidase B-like enzyme inhibits fibrinolysis *(22)*.

[†] Supported by grants HL-13423 (to F.J.C.) and HL-25942 (to A.T.) from the National Institutes of Health, and the Kleiderer/Pezold family endowed professorship (to F.J.C.).

[‡] The coordinates of $K5_{HPg}$ have been deposited in the Brookhaven Data Bank, access no. 5HPG.

* To whom to address correspondence.

[§] University of Notre Dame.

[∥] Michigan State University.

[1] Abbreviations: HPg, human plasminogen; HPm, human plasmin; $K1_{HPg}$, $K2_{HPg}$, $K3_{HPg}$, $K4_{HPg}$, and $K5_{HPg}$, the kringle 1 (residues C^{84}-C^{162}), kringle 2 (residues C^{166}-C^{243}), kringle 3 (residues C^{256}-C^{333}), kringle 4 (residues C^{358}-C^{435}), and kringle 5 (residues C^{462}-C^{541}) regions of human plasminogen, respectively; uPA, urokinase-type plasminogen activator; $K2_{tPA}$, the kringle 2 region (residues C^{180}-C^{261}) of tissue-type plasminogen activator; K_{uPA}, the kringle region (residues C^{50}-C^{131}) of human urokinase; Lp(a)-K4−37, kringle #37 of lipoprotein a, which is homologous to the kringle 4 domain of human plasminogen; MAb, monoclonal antibody; t-AMCHA, *trans*-4-aminomethylcyclohexane-1-carboxylic acid; 5-APnA, 5-aminopentanoic acid; EACA, 6-aminohexanoic acid; 7-AHpA, 7-aminoheptanoic acid; PnA, 5-aminopentane; HxA, 6-aminohexane; LBS, lysine binding site; PCR, polymerase chain reaction; TOF-MALDI-DE-MS, time-of-flight matrix-assisted laser-desorption−ionization with delayed-extraction mass spectrometry; T_m, temperature of maximum heat capacity; wt, wild-type; r, recombinant.

S0006-2960(97)02284-8 CCC: $15.00
Published on Web 02/20/1998

The HPg kringles possess different affinities and different specificities for ω-amino acid ligands. The tightest binding site for EACA is provided by $K1_{HPg}$ *(23, 24)*, followed by $K4_{HPg}$ *(23, 25, 26)*, and $K5_{HPg}$ *(26, 27)*. The $K3_{HPg}$ module does not interact with EACA to a measurable extent, whereas $K2_{HPg}$ displays a very weak interaction with this ligand *(28)*. Due to its high K_d value, it remains to be determined whether this latter site is of functional significance. Binding studies with a variety of ligands show that the affinities for $K1_{HPg}$ of a series of straight-chain ω-amino acid analogues proceeds through the order 5-APnA<EACA>7-AHpA *(24)*, whereas for $K4_{HPg}$ the order of affinity for these analogues is 5-APnA=EACA>7-AHpA *(25)*. In the case of $K5_{HPg}$, the relative binding efficacy for these ligands is similar to that found in $K1_{HPg}$, but their absolute K_d values are approximately an order of magnitude higher *(26)*. These examples show that the ω-amino acid binding sites in the HPg kringles possess significant differences.

Detailed steric relationships of the ligand and amino acid side chains of the HPg kringles have been delineated by X-ray crystallographic analyses of the EACA and t-AMCHA complexes of $K1_{HPg}$ *(29)*, and of EACA bound to $K4_{HPg}$ *(30)* and to a $Met^{66}Thr$ mutant of Lp(a)-K4−37 (unpublished results). Solution models of ligand binding have also been developed through NMR investigations of ligand/kringle complexes *(31−33)*, and through study of the characteristics of the ligand binding sites of recombinant variants generated by site-directed mutagenesis of $K1_{HPg}$ *(24)*, $K4_{HPg}$ *(26)*, and $K5_{HPg}$ *(26)*. To now, the three-dimensional structure of $K5_{HPg}$ has not been determined. Our interest in this structure is grounded in the fact that this kringle module possesses a significantly weaker affinity binding site for ω-amino acids and a stronger affinity for alkylamines than other HPg kringles *(26, 27, 34)*. We believed that the molecular basis of the ligand binding properties of $K5_{HPg}$ would be revealed through analysis of its three-dimensional crystal structure and through the generation of rationally designed mutants based on the structure. Accordingly, our two laboratories have collaborated in the investigation of these topics, and the results obtained constitute the subject of this report.

MATERIALS AND METHODS

Proteins and Polypeptides. Bovine fXa was provided by Enzyme Research Laboratories, Inc. (South Bend, IN). Restriction endonucleases were purchased from the Fisher Scientific Company (Springfield, NJ). Recombinant *Pfu* DNA polymerase was a product of Invitrogen (San Diego, CA). T4 DNA ligase was obtained from New England Biolabs (Beverly, MA).

Construction of the cDNA Expressing Wild-Type and Mutated $K5_{HPg}$. A full description of the plasmid containing the entire coding sequence of HPg, pUC118[Pg], has been provided earlier *(35)*. The basic strategy in constructing the target plasmid, pPIC9K[$K1_{Pg}$-IEGR-$K5_{HPg}$], was to amplify separately by PCR the $K1_{HPg}$ and $K5_{HPg}$ regions of the HPg cDNA with a linker containing bases that encode the fXa recognition cleavage site (Ile-Glu-Gly-Arg). A third PCR step served to ligate these two fragments.

Specifically, the $K1_{HPg}$ region of pUC118[Pg] was amplified by PCR with primers 1 and 2, below.

1. 5′-Forward Primer, 5′-GAT C′CT AGG TCA GAG TGC AAG ACT GGG. This primer encodes the sequence, Pro-Arg-Ser-Glu-Cys^1-Lys-Thr-Gly (Cys^1 is the first residue of $K1_{HPg}$), and includes the *Avr*II recognition site (underlined). After *Avr*II-catalyzed cleavage at C′ and insertion of the product into the same restriction site of the *Pichia pastoris* transfer vector, pPIC9K, the initial bases restore the 3′-end of the polylinker site of the transfer vector and the next two amino acids, Ser-Glu, flank the first cysteine residue of $K1_{HPg}$. The next three amino acids are residues 2−4, Lys-Thr-Gly, of $K1_{HPg}$.

2. 3′-Reverse Primer, 5′-TGC ATT GGA TCT TCC TTC GAT ATC ACA CTC AAG A. This primer encodes the C-terminus of $K1_{HPg}$ that also includes the recognition site (Ile-Glu-Gly-Arg, double underline) for fXa-catalyzed cleavage, upstream of which are codons for four amino acids from the C-terminus of $K1_{HPg}$, Leu-Glu-Cys^{79}-Asp (Cys^{79} is the last residue of $K1_{HPg}$). Downstream of the fXa-recognition sequence are codons for the first three amino acids, Ser^{-4}−Asn-Ala, of the $K5_{HPg}$ construct.

The $K5_{HPg}$ domain of pUC118[Pg] was amplified by PCR with oligonucleotide primers 3 and 4, below:

3. 5′-Forward Primer, 5′-GGA AGA TCC AAT GCA GAC TGT ATG TTT GGG. The 5′-terminus of this primer provided six bases (double underline) that anneal to the fXa-recognition site at the 3′-end of the $K1_{HPg}$ construct, followed by the codons for the N-terminus of $K5_{HPg}$, *viz.*, Ser-Asn-Ala-Asp-Cys^1-Met-Phe-Gly (Cys^1 is the first residue of $K5_{HPg}$).

4. 3′-Reverse primer, 5′-ATGCGGCCGC TTA CTA AGC AGC ACA CTG AGG GAC. Primer 4 placed a *Not*I restriction site (single underline) at the 3′-terminus of the cDNA for $K5_{HPg}$. This latter restriction endonuclease recognition sequence is preceded immediately upstream by two stop codons, TAA and TAG. Upstream of these stop signals are the codons for the C-terminus of $K5_{HPg}$, Val-Pro-Gln-Cys^{80}-Ala-Ala (Cys^{80} is the last residue of $K5_{HPg}$).

The cDNAs encoding the $K1_{HPg}$ and $K5_{HPg}$ domains were then annealed through overlapping bases in the fXa recognition site region and subjected to a third PCR step with primers 1 and 4. After restriction enzyme digestion and religation, the final plasmid, pPIC9K[$K1_{Pg}$-IEGR-$K5_{HPg}$], was obtained.

The insert in this plasmid was subjected to nucleotide sequence analysis to confirm its integrity.

Oligonucleotide-Directed Mutagenesis. The codon for Leu^{71} was altered to arginine using PCR. The sequences of the pairs of oligonucleotides employed in this procedure were (the mutagenic bases are provided in small lettering) as follows.

5. 5′-Forward Primer, 5′-CG ACA AAT CCA AGA AAA cgt TAC GAC TAC TGT G.

6. 3′-Reverse Primer, 3′-GC TGT TTA GGT TCT TTT gca ATG CTG ATG ACA C.

These primers encode the region Thr^{65}-Cys^{75}, and mutate Leu^{71} to arginine.

The following two additional oligonucleotides were used for all PCR reactions as 5′ and 3′-end primers.

7. 5′-CGTAGAATTCCCTAGGTC.

8. 5′-GAAGGTCTAGATGCTCACC.

Primers 7 and 8 incorporate *Eco*RI and *Xba*I sites (underlined) at the 5′- and 3′- ends, respectively, of the final PCR product.

To construct the entire mutated plasmid, pPIC9K[$K1_{Pg}$-IEGR-$K5_{HPg}$/$L^{71}R$], using these primers, a PCR-based strategy was employed, as follows. In two separate steps, primers 5 and 7 and 6 and 8, were annealed to plasmid pPIC9K-[$K1_{Pg}$-IEGR-$K5_{HPg}$], and each was extended using PCR with *Pfu* DNA polymerase. This step yielded PCR products of 511 bp and 867 bp, respectively. Using both PCR products together as templates for a third PCR step with primers 7 and 8 resulted in a PCR product containing 1346 bp, which possessed the desired mutation. This cDNA was treated with *Eco*RI/*Xba*I and ligated into the same unique restriction sites of pPIC9K, thus providing the final yeast transfer plasmid, pPIC9K[$K1_{Pg}$-IEGR-$K5_{HPg}$/$L^{71}R$]. This material was used for transformation of *Pichia pastoris* GS115 cells.

Nucleotide sequence analysis of the entire insert was conducted to confirm its genetic integrity.

Expression and Purification of the Fusion Polypeptide, $K1_{Pg}$-IEGR-$K5_{HPg}$. The transfer plasmids pPIC9K[$K1_{Pg}$-IEGR-$K5_{HPg}$] and pPIC9K[$K1_{Pg}$-IEGR-$K5_{HPg}$/$L^{71}R$] were linearized with restriction endonuclease *Sac*I and used for transformation via homologous recombination of *P. pastoris* strain GS115 by electroporation. Our selection procedures for isolation of appropriate Mut^+ multicopy His^+/GS115 clones for large-scale fermentation have been published *(36, 37)*. An extensive description of the procedures used for high bio-mass fermentation of the selected yeast clones have appeared in earlier works *(36, 37)*.

Purification on lysine-Sepharose of wtr-$K5_{HPg}$ was accomplished by affinity chromatography as described earlier for other kringle domains *(37)*. The $K1_{HPg}$-IEGR-$K5_{HPg}$ construct was then cleaved for 6 h at room temperature using bovine fXa as the catalyst, at a peptide:enzyme ratio of 50:1 (w:w). The digest was then applied to a lysine-Sepharose column (10 mL) that was equilibrated and subsequently washed with a buffer consisting of 50 mM Tris-HCl/50 mM NaCl, pH 7.7. The target, wt-$K5_{HPg}$, appeared in the wash, only slightly retarded by the column. After the baseline absorbance (280 nm) decreased to <0.05, EACA (20 mM, final concentration) was added to the wash solution, after which the $K1_{HPg}$ was eluted.

A slightly different scheme was employed to purify r-$K5_{HPg}$[$L^{71}R$]. Due to the enhanced binding of the ligand to the LBS of this mutant, r-$K5_{HPg}$[$L^{71}R$] did not wash through the column and coeluted with $K1_{HPg}$ after application of the above EACA solution. To resolve these two kringles from the fXa-digested tandem kringle construct, a gradient of EACA (start solution, 50 mM Tris-HCl/50 mM NaCl/0.02 mM EACA, pH 7.7; limit solution 50 mM Tris-HCl/50 mM NaCl/0.25 mM EACA, pH 7.7) was applied to a larger (60 mL) Sepharose-lysine column. With this approach, the r-$K5_{HPg}$ mutant appeared after elution of $K1_{HPg}$ and was clearly resolved from it. Approximately 10% of the sample was sacrificed in the elution region between the two kringles.

Crystallization. Initial incomplete factorial searches with *Hampton Crystal Screen* I using concentrations of 10 and 20 mg/mL of kringle yielded crystalline precipitates with only three of the conditions. Efforts to enlarge the crystals were unsuccessful. Previous experience with crystallization of kringles *(29, 38−41)* suggested that PEG 400 to PEG 8000 in Na^+-Hepes buffer, pH 7, with or without salt, would be more suitable for initial trials. An in-house set of factorial solutions utilizing Li_2SO_4 as salt (protein concentration of 60 mg/mL) produced small crystals of apo-$K5_{HPg}$ using the vapor diffusion hanging drop method, from a solution of 24% (w/v) PEG 8000/0.1 M sodium-Hepes, pH 7.0/0.15 M Li_2-(SO_4). The reservoir contained 1 mL of the solution, and the hanging drop consisted of 1 μL of the protein solution added to 1 μL of the reservoir solution. X-ray diffraction quality crystals with dimensions of 0.30 mm × 0.15 mm × 0.05 mm were obtained by multiple macroseeding while the PEG 8000 concentration was decreased from 24% to 22% to 18% to 16%.

Intensity Data Collection. The X-ray diffraction data of apo-$K5_{HPg}$ were collected with an R-AXIS II imaging plate detector using Molecular Structure Corporation-Yale focusing mirrors and CuKα radiation generated from a Rigaku RU200 rotating anode operating at 5 kW power with a fine focus filament (0.3 mm × 3.0 mm). Measurement of the intensity data was conducted at −150 °C using a cryosolvent solution consisting of 20% glycerol/20% PEG 4000/0.1 mM Na^+-Hepes, pH 7.0. The crystal-detector distance was 10 cm, and the detector-swing angle was 12.0°. Autoindexing and processing of the measured intensity data were carried out with the Rigaku R-AXIS software package *(42)*.

Structure Determination. The crystal structure of apo-$K5_{HPg}$ was determined by the molecular replacement method using the coordinates of apo-$K1_{HPg}$ *(43)* as an initial model. All residues of $K1_{HPg}$ that differed in sequence from apo-$K5_{HPg}$ were replaced with alanine in the model and the interkringle peptide and $K5_{HPg}$-catalytic domain tripeptide linker were ignored. Rotation/translation searches were carried out with the program AMoRe *(44)* in the range 10.0−3.0 Å resolution. The rotation search provided two solutions with correlation coefficients of 0.28 and 0.19, corresponding to the two molecules in the asymmetric unit related by a noncrystallographic 2-fold rotation axis approximately parallel to the *z*-direction. The two solutions were also in agreement with the self-rotation solution. The position of one molecule of the rotated structure was determined with a translation function that provided an *R*-value of 46.8% (correlation coefficient, 0.31); *R* was 50.1% (correlation coefficient, 0.18) for the other molecule. The coordinates of a model of both rotated molecules were optimized by rigid-body refinement to a *R*-value of 38.1% (correlation coefficient, 0.59). Additional positional refinement was conducted with the X-PLOR program package *(45)* by energy minimization to relieve close contacts of the model. This decreased the *R*-value to 33.5%.

Structure Refinement. The dimeric structure of apo-$K5_{HPg}$ was refined with the program PROLSQ *(46)* and PROFFT *(47)*. The first stage of the refinement, 7.0−2.8 Å, employed tight positional noncrystallographic symmetry (NCS) and an overall *B*-factor. After three cycles, starting with an average $B = 15.0$ Å^2, *R* only changed from 35.7 to 34.5%. The next three cycles of individual *B*-refinement with tight NCS geometry and temperature factor restraints for atoms of both the main chain and side chains (0.5 Å, 3.0 Å^2), and six cycles with looser NCS geometry and temperature factor restraints on side chains (1.0 Å, 10.0 Å^2), converged at $R = 31.9\%$.

Refinement using alternate tight-loose NCS restraints decreased *R* to 26.5%. At this stage, the ($2F_o - F_c$) electron and ($F_o - F_c$) difference density maps had most of the side chains of apo-$K5_{HPg}$ that were alanine residues in the initial

model. The insertion residue with respect to $K1_{HPg}$ was fixed based on the analysis of the electron and difference density maps after deletion and then reconstruction of the His^{33}-Thr^{37} region. This clearly showed that the insertion was Ser^{34}. Further refinement was conducted including most of the apo-$K5_{HPg}$ residues in the model. Solvent water molecules were found and added periodically, by examining difference density maps, during the refinement at 2.5 Å and higher resolution. In the final stage, beyond 2.1 Å resolution, the NCS restraints were abandoned and the two molecules of apo-$K5_{HPg}$ were refined independently.

Intrinsic Fluorescence Titrations. The binding of ω-amino acid ligands to r-$K5_{HPg}$ and its variants was measured as previously described by titration of the alteration in intrinsic fluorescence change in the kringle that occurred upon ligand binding *(24*, *26*, *37*). The experiments were carried out at 25 °C in a buffer containing 50 mM Tris-OAc/150 mM NaOAc, pH 8.0. The K_d values that characterize the ligand/kringle interaction were calculated from the fluorescence titrations by nonlinear least-squares iterative curve fitting of the titration data *(24*).

Differential Scanning Calorimetry. The samples were equilibrated by dialysis with 100 mM sodium phosphate, pH 7.4, or 50 mM sodium phosphate/50 mM EACA, pH 7.4. Thermograms were obtained employing a Nano Differential Scanning Calorimeter (Calorimetry Sciences Corporation, Salt Lake City, Utah). Thermal denaturation scans were conducted at 1 °C/min between the temperature range of 25−100 °C. The baseline for each run was obtained in an identical experiment with the buffer in each cell. The T_m values were determined using computer software that accompanied the equipment. The T_m values were independent of the scan rates under the conditions described.

^1H NMR. Samples were dissolved in 0.05 M sodium phosphate, pH 7.4, that was fully preexchanged with ^2H_2O. These solutions were lyophilized and then redissolved in the same volume of ^2H_2O. This exchange was repeated three additional times.

Homonuclear one-dimensional ^1H NMR spectra were obtained at 37 °C on a Varian (Palo Alto, CA) UNITY Plus 600 MHz Spectrometer in the Fourier mode with quadrature detection. Details of the methodology have been described previously *(37*, *48*). Chemical shift resonances are reported in δ (ppm) referenced to 4,4-dimethyl-4-silapentane-1-sulfonate, which was set to 0 ppm.

DNA Methodology. All methods used for DNA manipulations, which included oligonucleotide synthesis, cell transformations, plasmid minipreparations, PCR, and purification of DNA fragments have been described in previous publications from this laboratory *(24*, *48*, *49*). Nucleotide sequences were determined using the Automated Laser Fluorescent (ALF) Express DNA sequencer (Pharmacia Biotech, Piscataway, NJ), employing Cyp-5′ dATP labeling. All sequencing reagents were purchased from Pharmacia Biotech.

Peptide Analytical Methods. Molecular weights of the polypeptide samples were measured by MALDI-TOF-DE-MS on a Voyager-DE spectrometer (PerSeptive Biosystems, Framingham, MA) in the delayed extraction mode as previously described *(37*).

Automated solid state amino-terminal amino acid sequence analyses were accomplished as published previously *(50*).

RESULTS

A cDNA construct containing the recombinant $K5_{HPg}$ domain has been generated, wherein the $K5_{HPg}$ module has been linked to $K1_{HPg}$ via a fXa-catalyzed cleavage site. The rationale for employing this particular construct is based on the ease of purification on a lysine-Sepharose column of the weak lysine binding $K5_{HPg}$, when $K5_{HPg}$ is combined with the high binding affinity $K1_{HPg}$ domain. After a 17.5 h fermentation of the *Pichia pastoris* cells containing this construct in a high bio-mass fermentor, the polypeptide was purified from expression medium in a single step on the affinity column in a yield of approximately 150 mg/L. The wtr-$K5_{HPg}$ was then liberated from the tandem kringle construct by fXa-catalyzed cleavage of the linker region between the two kringles, and separated from $K1_{HPg}$ by rechromatography on the same lysine-Sepharose column. In this second chromatography step, wtr-$K5_{HPg}$ was only slightly retarded by the resin and appeared in the column wash buffer uncontaminated by r−$K1_{HPg}$, which remained bound to the column. Analysis by MALDI-TOF-DE-MS revealed the molecular mass of $K5_{HPg}$ to be 9555.6 Da (calculated, 9552.6 Da). This corresponds to within 3 mass units of the expected construct, SNAD[$K5_{HPg}$]AA, where [$K5_{HPg}$] represents residues Cys^1-Cys^{80} of this kringle domain (residues Cys^{462}-Cys^{541} of HPg). Correspondingly, amino-terminal amino acid sequence of the isolated $K5_{HPg}$ was determined to be Ser-Asn-Ala-Asp-Cys^1-Met-Phe-Gly-Asn-Gly-Lys-Gly-Tyr-Arg-Gly-Lys-Arg-Val-Thr-Thr-Val-Thr (where Cys^1 is the first residue of $K5_{HPg}$). This sequence matches the cDNA predictions over the entire amino-terminal 22 residues examined, except in one location, Val^{14}, which is encoded as an alanine in a previously reported HPg cDNA sequence *(51*), and in the amino acid sequence of human plasma HPg *(6*)[2]. However, a codon for valine is found in the nucleotide sequence of our construct and in our parent HPg cDNA, and may represent a polymorphism in HPg at this location. In any case, this conservative substitution is completely removed from the ligand binding site and plays no role in this particular property of $K5_{HPg}$.

Further characterization of this wtr-$K5_{HPg}$ was accomplished by DSC and ^1H NMR. Using the former method, the T_m that characterizes the thermal denaturation of this polypeptide was found to be 46.4 °C, which was shifted to 57.5 °C in the presence of saturating concentrations of EACA (Figure 1A). These values are in good agreement with those previously established for this kringle domain *(52*). Examination of the methyl proton region of the one-dimensional ^1H NMR spectrum of wtr-$K5_{HPg}$ clearly showed the strongly upfield-shifted $CH_3^{\delta'}$ protons of Leu^{46} at a value of −1.07 ppm. This major signal of proper kringle folding demonstrates that, like other isolated kringle domains previously studied, wtr-$K5_{HPg}$ adopts its proper folded conformation. These Leu^{46} protons are coupled to the CH_3^{δ} protons of Leu^{46} and the CH^{γ} proton of this same leucine residue, at chemical shift values of 0.35 and 1.09 ppm, respectively.

X-ray diffraction data from the crystal of apo-$K5_{HPg}$[3] were used to determine the unit cell as orthorhombic, space group

[2] Early in the crystallographic refinement, the ($2F_o - F_c$) and ($F_o - F_c$) electron density of Ala^{14} corresponded to threonine or valine in both $K5_{HPg}$ molecules. The placement of valine at position 14 was then confirmed by both amino acid and nucleotide sequence determinations.

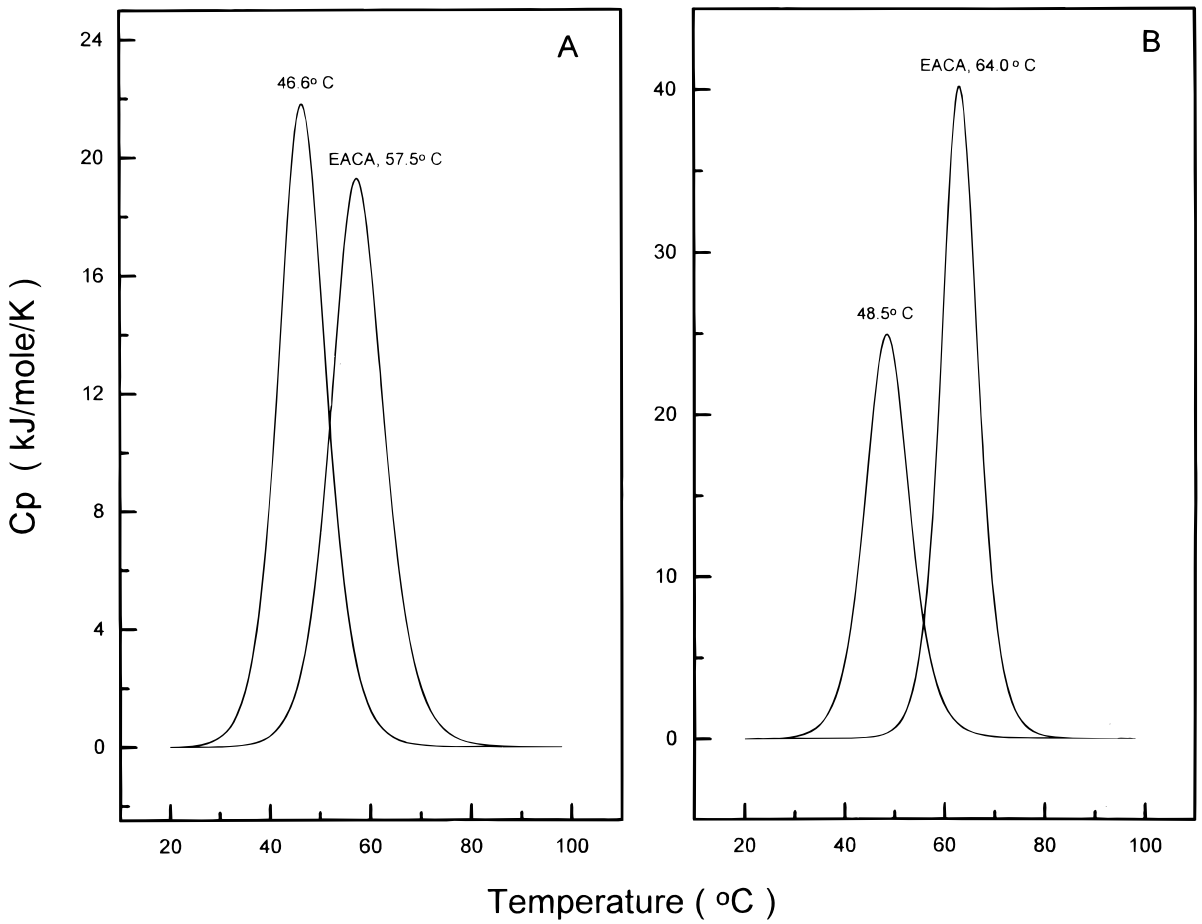

FIGURE 1: DSC thermograms of wtr-K5$_{HPg}$ and r-K5$_{HPg}$[L^{71}R] and their changes as a result of addition of EACA. The heat capacity at constant pressure (C_p) is plotted against the temperature. The buffers employed were 100 mM sodium phosphate, pH 7.4, or 50 mM sodium phosphate/50 mM EACA, pH 7.4. The temperature of maximum heat capacity (T_m) for each sample is indicated on the graph in the absence and presence of EACA. The concentrations of the peptides were approximately 0.5 mg/mL. (A) wtr-K5$_{HPg}$. (B) r-K5$_{HPg}$[L^{71}R].

$P2_12_12$, with dimensions of 77.43 Å (a) × 79.20 Å (b) × 30.78 Å (c). The asymmetric unit contained two molecules of apo-K5$_{HPg}$ related by a noncrystallographic 2-fold rotation axis approximately parallel to the z-direction. The intensity data collection statistics are summarized in Table 1. These were further used to obtain the model of apo-K5$_{HPg}$ shown in Figure 2. The refinement parameters and their deviations are listed in Table 2. The final model converged at an R-value of 16.6% at 1.66 Å resolution, and consisted of 1294 protein atoms[4] and 193 water molecules with occupancy >0.6. The RMSD between the superimposed CA atoms of the two apo-K5$_{HPg}$ kringles is 0.31 Å. The Ramachandran plot of the two kringles is shown in Figure 3, where it is observed that there is close coupling of the φ,ψ angles of the two molecules. The interface between the 2-fold related kringles consists of an antiparallel arrangement of Leu^{71}-Pro^{83} segments of the C-terminus of each kringle molecule (Figure 4). Of the 34 water molecules hydrogen bonding to these two segments, seven hydrogen bond with both, mediating the dimeric interaction between the two K5$_{Hpg}$ molecules (Figure 5). Direct hydrogen-bonding interactions also occur between these regions in a 2-fold manner, near their ends, and involve Lys^{70}, Asp^{73}, and Ala^{82}. They also occur close to the 2-fold axis involving Asp^{76}, while seven hydrophobic residues from each molecule, respectively, participate in stabilizing nonpolar contacts (Figure 5).

Table 1: Crystal Data Collection of Apo-K5$_{HPg}$

cell constants (Å)	
a	77.43
b	79.20
c	30.78
space group	$P2_12_12$
molecules/asymmetric unit	2
solvent fraction (%)	42
excluding interkringle peptides	52
resolution (Å)	1.66
observations (I/σ > 1.0)	42 366
R-merge (%)	4.2
outermost range (1.80−1.66) Å	8.7
independent reflections (I/σ > 1.0)	16 720
redundancy	2.5
completeness (%)	72
outermost shell	37
I/σ (outermost range)	3.6

[3] The K5$_{HPg}$ used for the X-ray study (*26*) was a different construct from that described here for the mutagenesis experiments, in terms of the amino acids that flanked the kringle residues. However, the K5$_{HPg}$ residues were identical in both cases. No significant differences were present in the two wild-type constructs regarding ligand binding properties, calorimetric T_m values, and proton chemical shifts of the kringle residues.

[4] Although the first three residues, *viz.*, Ala-Ala-Pro, of the linker between K5$_{HPg}$ and the catalytic domain of HPg were well defined in the structure, the octadecapeptide interkringle link between K4$_{HPg}$ and K5$_{HPg}$ was disordered in solvent space of the crystal structure. This made the solvent component of the crystal appear to be more like 52%, rather than 42% (Table 1).

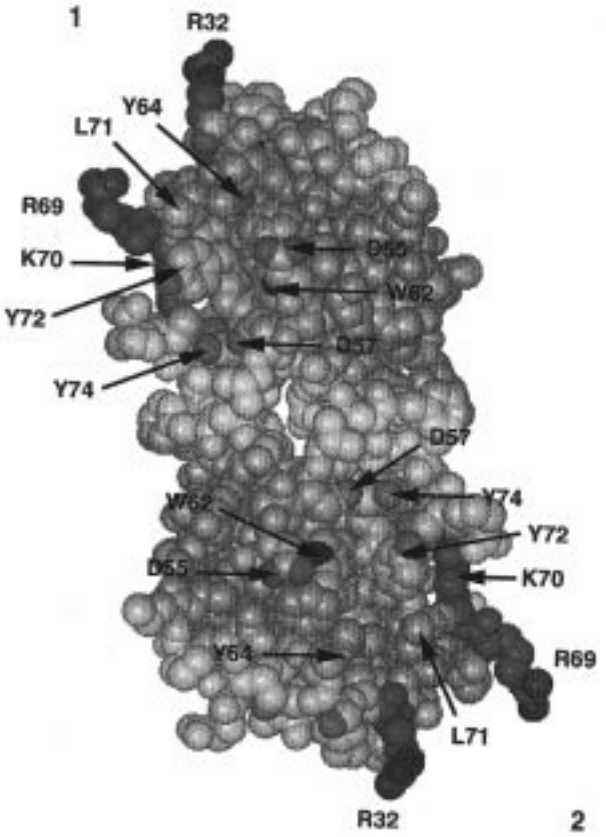

FIGURE 2: Space filling representation viewed approximately down the local 2-fold axis in the crystal structure of the apo-$K5_{HPg}$ dimer. Atoms of the regions of the structures defining the LBS, *viz.*, His^{33}-Thr^{37}, Pro^{54}-Val^{58}, Pro^{61}-Tyr^{64}, and Leu^{71}-Tyr^{74}, are in orange, except for the side chain atoms of oxygen (red) and nitrogen (blue) of these regions. Several pertinent residues in the putative LBS are labeled. The amino acids depicted with green carbon atoms are cationic residues that in other kringle domains serve to stabilize binding of the carboxyl group of the ligand. These residues are highlighted in this figure to show that they are not candidates for this same function in $K5_{HPg}$. In fact, Lys^{70} makes an important interaction with Pro^{83} of the adjoining kringle (see also Figures 4 and 5).

Table 2: Summary of Final Restrained Least-Squares Parameters[a]

	target	RMSD
distances (Å)		
bond lengths	0.020	0.016
bond angles	0.040	0.034
planar 1−4	0.060	0.050
planes (Å)		
peptides	0.030	0.032
aromatic groups	0.030	0.030
chiral volumes (Å^3)	0.130	0.160
nonbonded contacts (Å)		
single torsion	0.80[b]	0.18
multiple torsion	0.80[b]	0.24
possible H-bond	0.80[b]	0.23
thermal parameters (Å^2)		
main chain bond	1.5	1.4
main chain angle	2.0	1.7
side chain bond	3.0	3.5
side chain angle	3.5	4.1
R-factor (%)		16.6

[a] Diffraction pattern weight: $\sigma(|F_o|) = A + B(\sin\theta/\lambda - 1/6)$; $A = 16$, $B = -45$. Average B value = 15.4 Å^2. [b] Basically, no restraint.

Kringles have a propensity to naturally occur in tandem arrays *(1)* and associate with one another to form more compact units *(53, 54)*. The latter consideration also applies to crystal structures when more than one kringle molecule constitutes the asymmetric unit *(29, 55)*. Although a number of different arrangements utilizing local rather than crystallographic symmetry elements have been identified in crystal structures, such as 2-fold rotation axis and pseudo 2_1 and 3_1 screw axis-like symmetries, none correspond to the unique antiparallel C-terminal interface arrangement of $K5_{HPg}$, in which 389 Å^2 (13% of each kringle) of surface area is inaccessible to solvent. However, the most distinguishing characteristic of the $K5_{HPg}$ dimer, as compared to other kringles, is the large number of water molecules mediating the dimer interface. Whether this, or any of the other known kringle associations in crystals are physiologically relevant remains to be shown by structure determination of a tandem kringle array.

The LBS is defined by His^{33}-Thr^{37}, Pro^{54}-Val^{58}, Pro^{61}-Tyr^{64}, and Leu^{71}-Tyr^{74}, which together form an elongated depression on the kringle surface approximately 9 Å wide and 12 Å long (Figure 2) that is lined with solvent water molecules (Figure 6). The hydrogen bonds that occur in the LBS of $K5_{HPg}$ are provided in Table 3. Those listed from Asn^{53} to Thr^{65}, especially when involving water molecules, reflect the excellent 2-fold symmetry between two independent $K5_{HPg}$ molecules, the refinement of which concluded without NCS restraints. The 16 hydrogen bonds in each LBS strongly support the idea that the LBS of kringles is essentially preformed prior to, and independent of, ligand binding. In the case of molecule 1, Gln^{28}, Arg^{32}, and Ser^{34} from molecule 2 of a neighboring dimer make several hydrogen bonds that do not possess 2-fold symmetry because of local rather than crystallographic symmetry relationships between these contacts. The Arg^{32} of the neighbor (Figure 6) limits access to the LBS of molecule 1 in the crystal. However, in molecule 2, the LBS is essentially unobstructed. It is also noteworthy that the LBS of molecule 1 is systematically occupied by eight water molecules (Figure 6), while molecule 2, which lacks intermolecular contacts in this location, contains only five water molecules (not shown). In fact, the $(2F_o - F_c)$ electron density of seven of the water molecules in molecule 1 is connected at the 1σ level, resembling that of ligand binding. This apparent relationship to ligand binding is probably the result of the intermolecular interaction of the LBS with Gln^{28}, Arg^{32}, and Ser^{34} from the adjacent molecule(s), which decreases the thermal motion of the water molecules.

The segment, His^{33}-Thr^{37}, contains residue Ser^{34}, which, from structural superposition, is deleted in $K1_{HPg}$. This part of the kringle molecule appears to possess the most flexibility *(40, 56)* and represents the only region of the backbones of a number of kringle domains that differ from each other. Although the differences between CA atoms of Ser^{34} of the two apo-$K5_{HPg}$ molecules is 1.1 Å, the main and side chains of His^{33} and Phe^{36} compensate for this displacement of Ser^{34} and adopt the same orientation in both molecules (Figure 7). This is probably due to the hydrophobic edge-face interaction of Phe^{36} with Tyr^{64} and Trp^{62}, respectively. Residues Trp^{62}, Tyr^{64}, Tyr^{72}, and Tyr^{74} of the Pro^{61}-Tyr^{64} and Leu^{71}-Tyr^{64} segments are in orthogonal orientations to each other, also utilizing aromatic stacking interactions and forming a structural framework with hydrophobic regions of ligands (Figures 2 and 7).

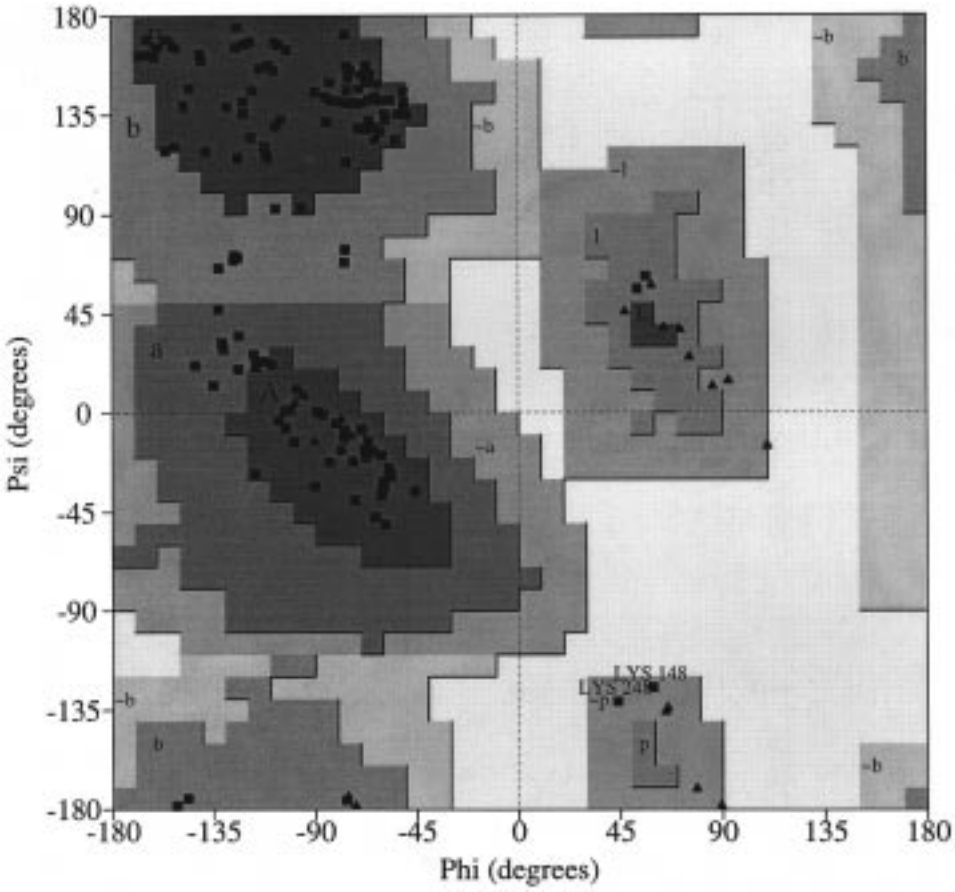

FIGURE 3: The Ramachandran plot of the final structure of the $K5_{HPg}$ dimer. Only Lys^{48} of molecules 1 and 2 is present in a "generously allowed region" (designated by ~p). The illustration was generated using PROCHECK *(67)*.

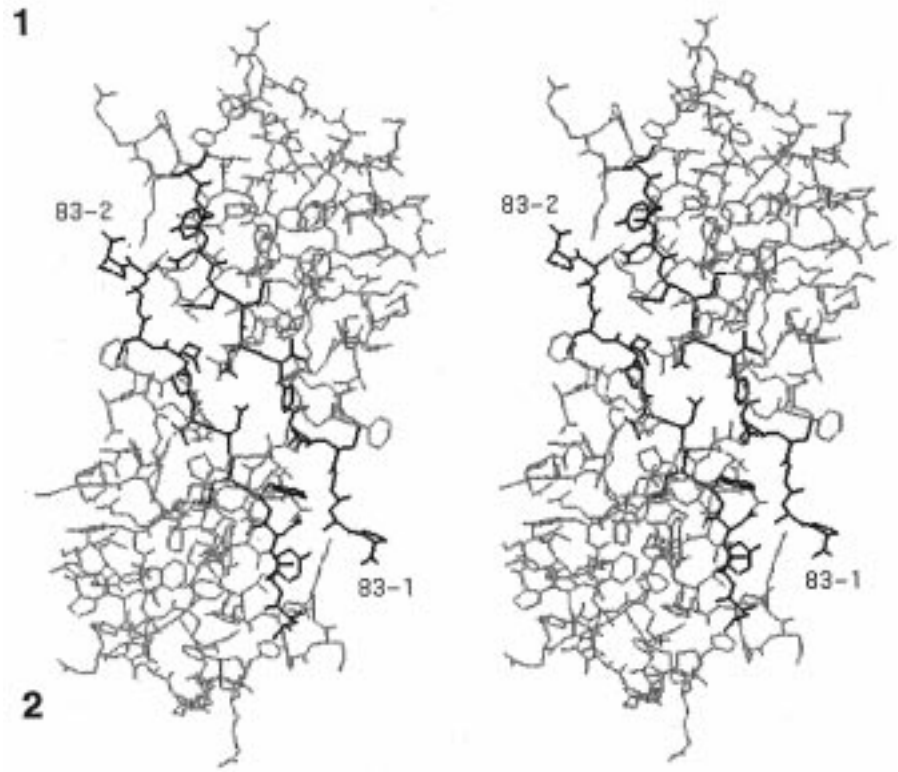

FIGURE 4: Stereoview highlighting the interfacial region between the two $K5_{HPg}$ kringles in the asymmetric unit viewed as in Figure 2. The regions in black depict residues 71−83 in molecules 1 and 2. Residue 83 is labeled in molecule 1 (83−1) and molecule 2 (83−2).

On the basis of similarities with $K1_{HPg}$ *(24, 29)*, $K2_{tPA}$ *(40, 49, 57)*, and $K4_{HPg}$ *(26, 30)*, the cationic residues of $K5_{HPg}$, *viz.*, Arg^{32}, Arg^{69}, and Lys^{70}, are candidates for interaction with the carboxylate of the ligand. However, as highlighted

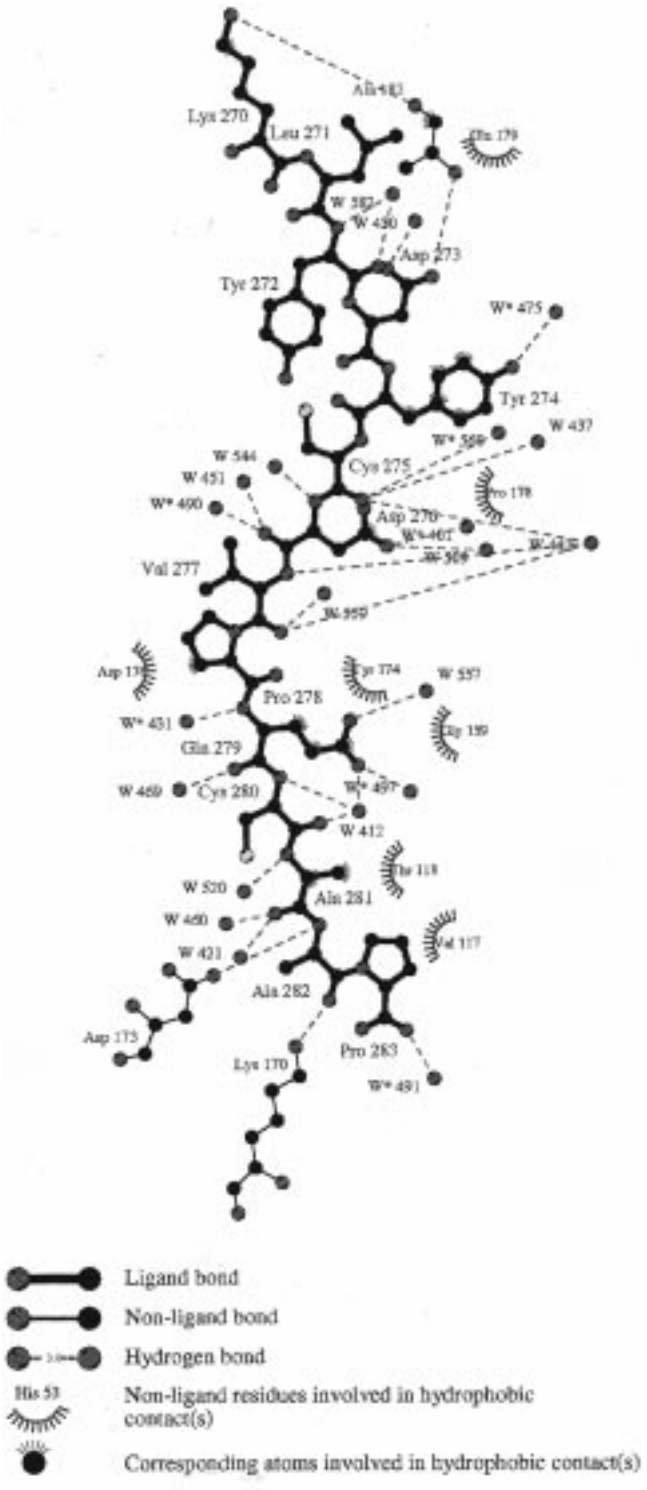

FIGURE 5: Schematic of interactions occurring in the dimer interface of $K5_{HPg}$. Hydrogen bonding interactions <3.0 Åare shown by broken lines; water molecules hydrogen bonding with both segments of dimer interface are designated as W*; 100 is added to residue number of molecule 1 and 200 is added to residues of molecule 2. The only interaction not displayed is a hydrogen bond between the carboxylate groups of Asp_{176} and Asp_{276}. Molecule 2 is taken to be the ligand.

in Figure 3, and shown in Figure 8, these residues are either clearly removed from the binding pocket of $K5_{HPg}$, and/or have unfavorable orientations for interaction with the ligand. This is also revealed by the distances of their functional groups from side chains of Asp^{55}, Asp^{57}, Trp^{62}, and Tyr^{72} residues that are uniformly critically positioned in the LBS in all other ligand binding kringles. Examination of all other cationic side chains of $K5_{HPg}$ shows that none can contribute to the putative ligand binding pocket, except possibly His^{33} (Figure 6). However, His^{33}-NE is hydrogen bonded to Trp^{25}-O. In order for this group to play a role as a cation donor to the ligand carboxylate moiety, the orientation of the imidazole would have to be repositioned by approximately 180°.

Titrations of the large change in intrinsic fluorescence accompanying the interaction of ligands with wtr-$K5_{HPg}$ have been utilized to determine K_d values that characterize the interaction of a variety of ω-amino acids with this polypeptide. The titration data provided in Figures 9 and 10 show the large and saturable changes (range −8% to −25% for the various ligands at saturation) in this property consequent to ligand binding. With data of this type, K_d values have been determined for the interaction of wtr-$K5_{HPg}$ and three straight-chain ω-amino acid analogues, 5-APnA, EACA, and 7-AHpA, as well as for the ring-based ligand, t-AMCHA, and the acarboxy straight-chain alkylamines, PnA and HxA. The values obtained are listed in Table 4.

To test the importance of Leu^{71} in the LBS, the recombinant mutant, r-$K5_{HPg}[L^{71}R]$, has been constructed, expressed in this same yeast system, and purified. The final product possessed a molecular mass of 9591.6 Da (calculated, 9595.7 Da) and an identical amino-terminal sequence through 25 residues as was found for wtr-$K5_{HPg}$. This mass spectral analysis demonstrates that the mutation was present in the purified product. Additionally, the T_m for thermal denaturation of r-$K5_{HPg}[L^{71}R]$ was 48.5 °C in the absence of EACA and 64.0 °C at saturating levels of this ligand (Figure 1B). Thus, while the native conformation of apo-r-$K5_{HPg}[L^{71}R]$ was only marginally more thermally stable than that of wtr-$K5_{HPg}$, a much larger degree of thermal stabilization of the native conformation of r-$K5_{HPg}[L^{71}R]$ resulted from ω-amino acid ligand binding than was the case with wtr-$K5_{HPg}$. This most likely reflects the different modes of ligand binding to these two r-$K5_{HPg}$ constructs. Also, regarding the nature of the conformation adopted by the $K5_{HPg}$ mutant, it was determined that the chemical shift values for side-chain Leu^{46} protons were −1.05, 0.36, and 1.10 ppm for the $CH_3^{\delta'}$, CH_3^{δ}, and CH^{γ} protons, respectively. These latter values were nearly identical with those displayed by wtr-$K5_{HPg}$, showing that this construct could be usefully employed for comparisons with wtr-$K5_{HPg}$ of its ligand binding properties.

Using intrinsic fluorescence titrations, the binding (dissociation) constants of r-$K5_{HPg}[L^{71}R]$ for 5-APnA, EACA, 7-AHpA, t-AMCHA, PnA, and HxA have also been determined. The magnitudes, and in the case of t-AMCHA, the sign, of the fluorescence changes possess some differences to those observed for wtr-$K5_{HPg}$ (Figures 9 and 10). This indicates that the environment of the residue reporting the changes, likely Trp^{62}, is not the same in the two ligand-bound kringles. Such dissimilarities could include the nature of the hydration of the LBS, the orientation of ligand in the binding pocket, and/or the nature of side-chain-reporter group contacts. Since the ligand must bind in the more hydrophilic pocket of the mutant quite differently than in the more hydrophobic site of its wild-type counterpart, the differencesin the intrinsic fluorescence of the ligand-saturated polypep-

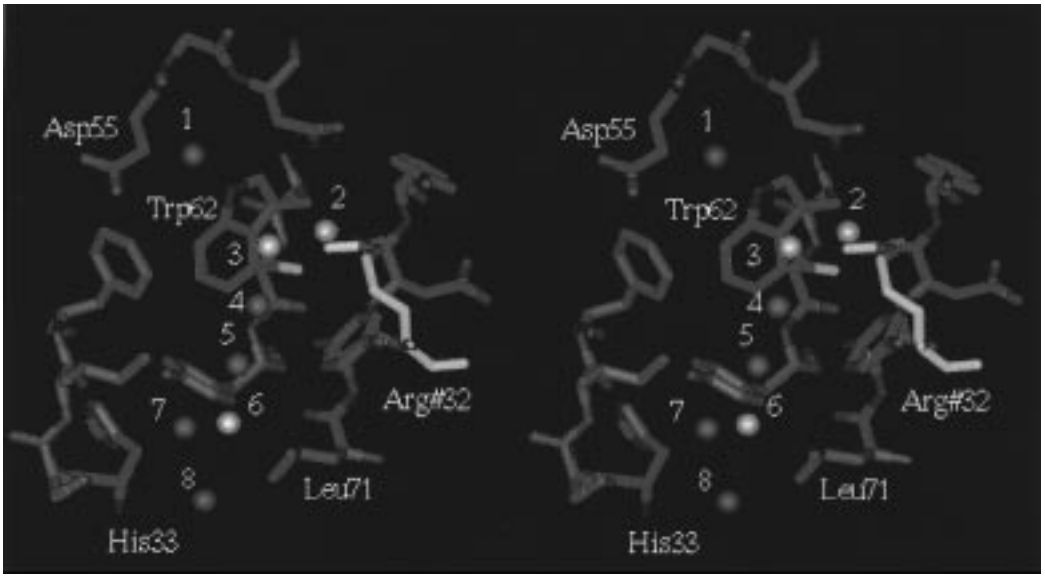

FIGURE 6: Stereoview of specific residues of apo-$K5_{HPg}$ potentially present in the LBS of molecule 1 of the $K5_{HPg}$ dimer. The regions of the kringle represented are His^{33}-Phe^{36}, Asp^{55}-Asp^{57}, Trp^{62}-Tyr^{64}, and Leu^{71}-Tyr^{74}. A residue of each segment is labeled. Carbon atoms are in green, nitrogens in blue, oxygens are colored red, and sulfur yellow. Shown with orange carbon atoms is Arg^{32} of molecule 2 of an adjacent $K5_{HPg}$ dimer, which is partly inserted in the binding pocket of molecule 1 of the $K5_{HPg}$ illustrated. Water molecules common to the LBS of both kringles of the dimer are red spheres; those in molecule 1, only, are in pink. 1 = O_w540, 2 = O_w525; 3 = O_w419; 4 = O_w565; 5 = O_w589; 6 = O_w524; 7 = O_w 526; 8 = O_w527 of the PDB coordinate file.

Table 3: Hydrogen Bonds in the Lysine Binding Site Region of $K5_{HPg}$

		molecule 1	molecule 2
Asn^{53}-OD1	Asp^{57}-N	2.84	2.83
-OD1	O_w540/470	2.93	2.97
-ND2	Asn^{5}-O	2.70	2.70
-ND2	Asp^{57}-O	2.97	2.94
Asp^{57}-OD1	Gly^{59}-N	2.81	2.93
-OD2	Gly^{60}-O	3.12	2.95
Pro^{61}-O	Cys^{75}-N	3.02	2.99
Trp^{62}-N	Arg^{52}-O	2.91	2.87
-O	-N	2.94	2.98
-NE1	O_w540/470	3.10	2.92
Cys^{63}-N	Asp^{73}-O	2.87	2.96
-O	-N	2.93	2.98
Tyr^{64}-N	O_w502/418	2.97	2.84
-O	Gln^{23}-N	2.61	2.81
-OH	O_w526/425	2.71	2.84
Thr^{65}-N	Lys^{71}-O	2.97	2.92
Tyr^{72}-N	Ser^{34}-OG[a]	2.90	
-O	Ser^{34}-OG[a]	2.55	
-O	O_w582[a]		2.76
-OH	O_w491[a]	2.64	
-OH	Gln_{28}-OE1[a]	2.81	
Tyr^{74}-OH	Arg^{32}-NH_2[a]	3.00	

[a] Neighboring molecule in crystal; hydrogen bond has no local 2-fold rotation equivalent.

tide are not surprising. In any case, this intrinsic fluorescence change is saturable for all of the ligands that exhibited binding, and, thus, can be effectively employed to monitor ligand−kringle interactions. Accordingly, the binding (dissociation) constants that characterize these interactions are provided in Table 4. Comparisons of the K_d values of the ligands to wtr-$K5_{HPg}$ and r-$K5_{HPg}$[$L^{71}R$] clearly demonstrate the enhanced binding of the ω-amino acids and the decreased affinity of alkylamines (by the lack of fluorescence changes) to this mutant kringle. The K_d values obtained for the ligand/r-$K5_{HPg}$[$L^{71}R$] interactions are also compared to those for other kringle domains in Table 4.

DISCUSSION

The X-ray crystal structure of $K5_{HPg}$ has been employed to examine critical aspects of the ligand binding pocket of this kringle. The affinities of typically studied ω-amino acids for this domain are weak, as compared to $K1_{HPg}$ and $K4_{HPg}$, and, as a result of this investigation, the reasons for this are now more clearly understood.

The presence of certain amino acid side chains have been shown to be essential for ligand binding to kringles. These have been inferred from the crystal structures of kringle domains *(29*, *30*, *40*, *58*, *59)* from solution structural studies utilizing NMR methodology *(60*−*62)* and more directly from site-directed mutagenesis analyses *(26*, *37*, *48*, *49*, *57*, *61*, *63*, *64)*. Focusing on the latter types of studies, it has been shown that two aspartic acid residues in similar locations to Asp^{54} and Asp^{56} of $K1_{HPg}$ are required for stabilization of the amino group of the ligand *(26*, *63)*. The other end of the binding pocket contains a basic residue that interacts with the carboxylate group of ω-amino acids: Lys^{33} in the case of $K2_{tPA}$ *(49*, *57)* or, in other kringles, residues equivalent to Arg^{70} of $K1_{HPg}$ *(26*, *64)*. Lining each side of the binding pocket are two critical aromatic residues, corresponding to Trp^{61} and Tyr^{71} of $K1_{HPg}$ *(26*, *37*, *48*, *64)*. While other amino acid side chains indirectly influence the ω-amino acid binding characteristics of kringles, such as those in analogous locations to Tyr^{63} *(49*, *64*, *65)* and Tyr^{73} *(64*, *66)* of $K1_{HPg}$, all of the diverse methods employed for analysis of this topic are in essential agreement that the residues referred to above are critical for integrity of ligand binding.

Considering the three-dimensional structure of $K5_{HPg}$, as in the cases of $K1_{HPg}$ and $K4_{HPg}$, the segment Pro^{54}-Val^{58} of apo-$K5_{HPg}$ contains the Asp^{55}/Asp^{57} pair. These two residues impart a negatively charged anionic center to the LBS, which is responsible in other kringle domains for the interaction with positively charged groups of binding ligands (Figure

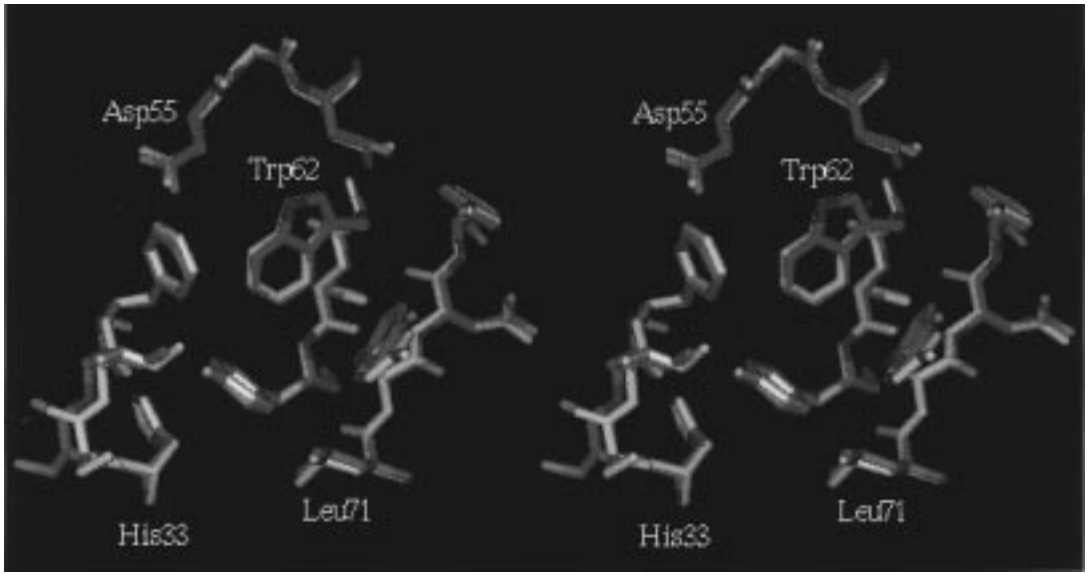

FIGURE 7: Stereoview of the superposition of the lysine binding sites of the independent $K5_{HPg}$ molecules of the dimer. A residue of each segment of the LBS is labeled. Molecule 1: carbon, green; nitrogen. blue; oxygen, red; sulfur, yellow. Molecule 2 is colored orange. In this latter case, individual atoms have not been distinctly colored, since this led to better clarity of the figure.

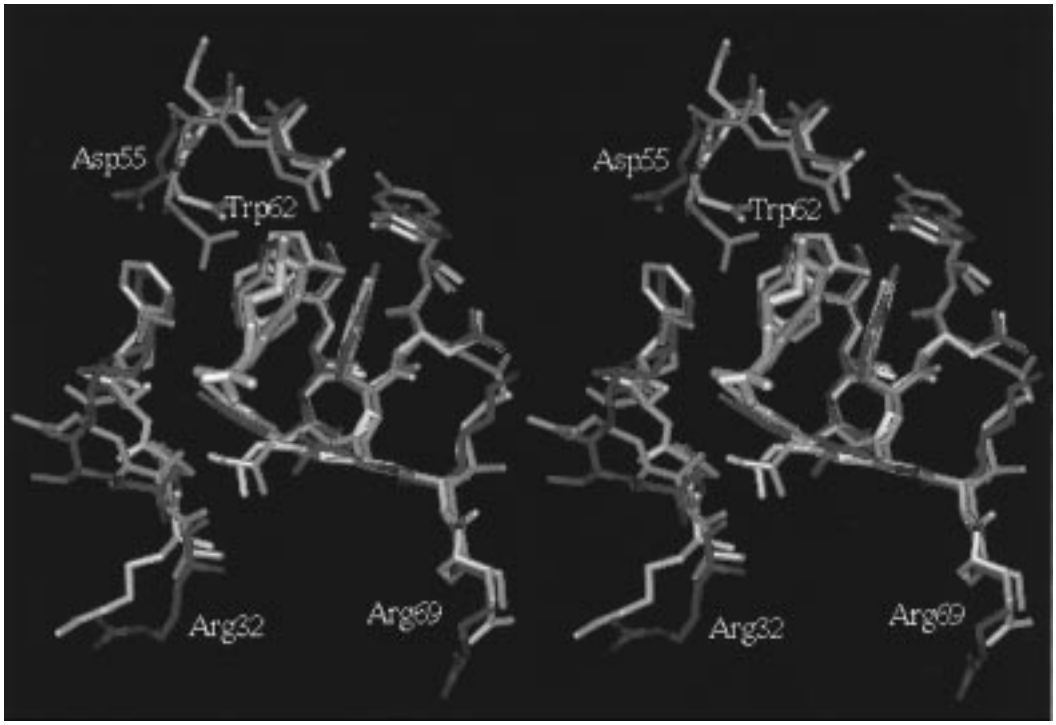

FIGURE 8: Stereoview of the superposition of the lysine binding site of the EACA complex of $K1_{HPg}$ and $K4_{HPg}$ on molecule 1 of $K5_{HPg}$. $K5_{HPg}$ is illustrated with the following atom colors: green for carbon, blue for nitrogen, red for oxygen, and yellow for sulfur. All atoms of $K1_{HPg}$ are shown in gray and those for $K4_{HPg}$ are in pink. EACA molecules are illustrated in the binding pockets in thicker lines. All residues numbered are according to $K5_{HPg}$.

8). However, in apo-$K5_{HPg}$, Asp^{55} resides in a different orientation ($\chi_1 \approx 100°$) than in other lysine binding kringles ($\chi_1 \approx 60°$), and extends toward solvent space (Figures 3, 7, and 8). This leads to an open conformation between the two aspartic acid residues, apparently nonconducive for ligand binding, and mitigates against an important functional role for Asp^{55} in this regard in $K5_{HPg}$. However, the regions Pro^{61}-Tyr^{64} and Leu^{71}-Tyr^{74} contain the requisite binding pocket aromatic residues, Trp^{62} and Tyr^{72}, which are positioned optimally for ligand binding (Figures 2, 6, and 8). The Asp^{55} residue could possibly reorient with ligand binding to form a doubly charged salt bridge with Asp^{57} and the amino group of the ligand, as is the case in other ligand binding kringles.

The unique feature of the LBS region of apo-$K5_{HPg}$ structure is the absence of a cationic center formed by the Lys^{35}/Arg^{71} and Arg^{34}/Arg^{70} pairs of $K1_{HPg}$ *(29)* and $K4_{HPg}$ *(30, 41)*, respectively. In apo-$K5_{HPg}$, residues positioned near these locations, *viz.*, Arg^{32}, Arg^{69}, and Lys^{70}, are not appropriately oriented in the binding pocket to serve a functional role in stabilizing ligand interactions (Figures 2 and 8). Since this region is responsible for the binding of negatively charged groups of ligands, the interaction between apo-$K5_{HPg}$ and ω-amino acid ligands is restricted to the

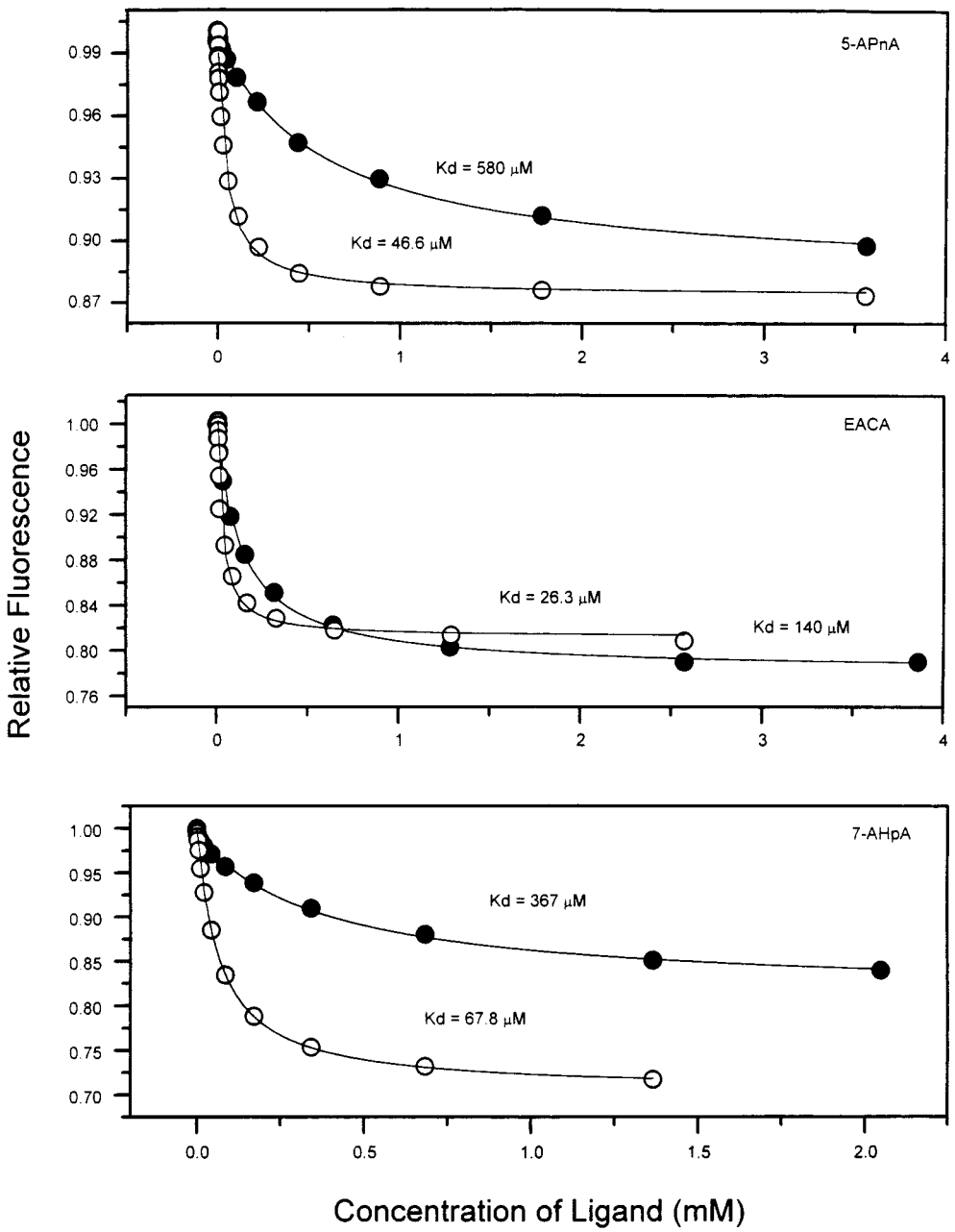

FIGURE 9: Binding of ligands to wtr-$K5_{HPg}$ and r-$K5_{HPg}[L^{71}A]$. Titrations of the change in intrinsic fluorescence of wtr-$K5_{HPg}$ (●) and r-$K5_{HPg}[L^{71}A]$ (○) with changes in the concentration of 5-APnA, EACA, and 7-AHpA are illustrated The intrinsic fluorescence in the absence of ligands was arbitrarily assigned an initial value of 1.0. The curves were fit by iterative nonlinear least-squares analysis to K_d values indicated in the panels. The starting buffer was 50 mM Tris-OAc/150 mM NaOAc, pH 8.0, at 25 °C.

positively charged groups of the ligands and the anionic center of the LBS, along with hydrophobic contacts in the binding pocket. Preference for such restricted interaction has already been observed for the EACA complex of a Met^{66}-Thr variant of Lp(a)-K4−37 *(59)*. In that case, the ϵ-amino group of EACA interacts with the anionic center and the carboxylate group of EACA, and extends into the solvent region perpendicular to the surface of the kringle and the LBS. Surprisingly, the ligand does not interact with the cationic center, although such a donor group is present. Ligands bound to the LBS usually lie on the surface of the kringle between the two charged centers separated by the aromatic region. We have recently crystallized the same mutant Lp(a)-K4−37/EACA complex from a more acidic solution (pH 4.5), in another crystal system, and determined its structure at 1.8 Å resolution (unpublished results). In this case, EACA is bound in the usual manner, as observed (Figure 8) with EACA/$K1_{HPg}$ *(29)* and EACA/$K4_{HPg}$ *(30)*.

When the backbones of two other ligand binding HPg kringles, $K1_{HPg}$ and $K4_{HPg}$, are superimposed and the steric relationships of ligands to critical amino acid side chains are examined and compared to $K5_{HPg}$, it is clear that the cationic center of $K5_{HPg}$ is isostructurally occupied by Leu^{71} (Figure 8). This unambiguous positioning of Leu^{71} afforded the opportunity to redesign the binding pocket by substituting an arginine residue for leucine at this sequence position. Thus, the mutant $K5_{HPg}[L^{71}R]$ was generated, and its ligand binding properties investigated.

Similar to experiments described above for wtr-$K5_{HPg}$, K_d values were determined for a variety of ligands for r-$K5_{HPg}$-$[L^{71}R]$ (Figures 9 and 10, and Table 4). The data show that all ω-amino acid ligands bind approximately 5−10-fold

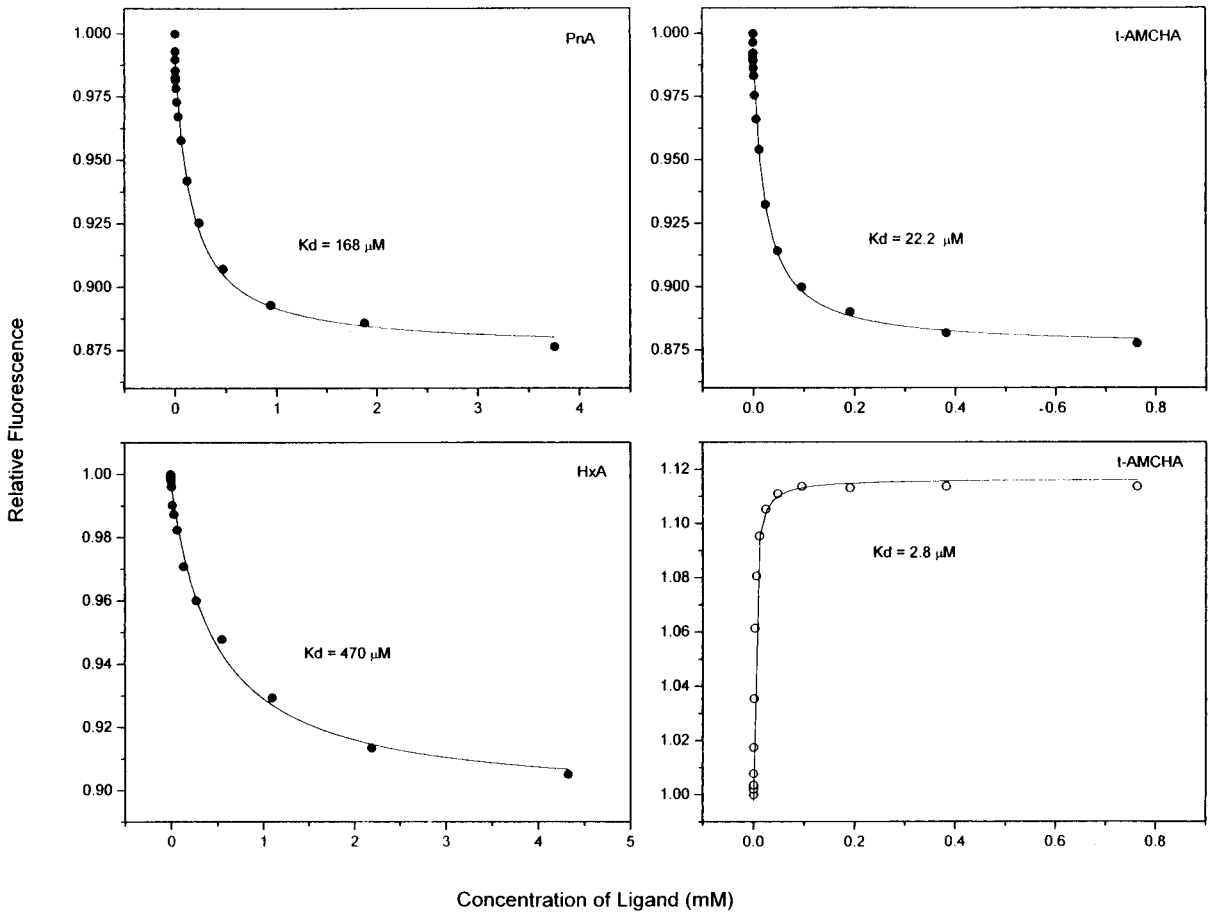

FIGURE 10: Binding of ligands to wtr-K5$_{HPg}$ and r-K5$_{HPg}$[L^{71}R]. Titrations of the change in intrinsic fluorescence of wtr-K5$_{HPg}$ (●) and r-K5$_{HPg}$[L^{71}R] (○) with changes in the concentration of PnA, HxA, and t-AMCHA are displayed; r-K5$_{HPg}$[L^{71}R] showed no fluorescence changes with PnA and HxA. The intrinsic fluorescence in the absence of ligands was arbitrarily assigned an initial value of 1.0. The curves were fit by iterative nonlinear least-squares analysis to the K_d values indicated in the panels. The starting buffer was 50 mM Tris-OAc/150 mM NaOAc, pH 8.0, at 25 °C.

Table 4: K_d Values for Ligand Binding to Wild-Type and Variant r-K5$_{HPg}$-Based Kringles

mutant	5-APnA (μM)	EACA (μM)	7-AHpA (μM)	t-AMCHA (μM)	PnA	HxA
wtr-K5$_{HPg}$	580	140	367	22	168 μM	470 μM
r-K5$_{HPg}$[L^{71}R]	47	26	68	3	nc[a]	nc[a]
wtr-K1$_{HPg}$[b]	24	12	250	1	nd[c]	nd[c]
K4$_{HPg}$[d]	29	26	280	5	3 mM[e]	nd[c]
wtr-K2$_{tPA}$	325[f]	43[g]	6[g]	9[g]	nd[c]	nd[c]

[a] No fluorescence change. [b] Data from ref 24. [c] Not determined. [d] Data from ref 25. [e] Data from ref 27. [f] Unpublished data, V. S. De Serrano. [g] Data from ref *57*.

tighter to this mutant than to its wild-type parent. Thus, a highly significant increase in affinity of the ligand for its binding site on K5$_{HPg}$ accompanies this single substitution, to the extent that the K_d of EACA for r-K5$_{HPg}$[L^{71}R] is essentially the same as that of this ligand for K4$_{HPg}$ and only 2-fold weaker than the best affinity of EACA (for K1$_{HPg}$). In addition, the K_d values of the ligands specified in Table 4 do not respond similarly to the mutation in K5$_{HPg}$, leading to unique characteristics of ligand binding to r-K5$_{HPg}$[L^{71}R]. This is principally reflected in the relative affinity 7-AHpA for this variant kringle. This ligand binds more tightly to r-K5$_{HPg}$[L^{71}R] than to any of the other HPg kringles, while binding affinities of 5-APnA and EACA for r-K5$_{HPg}$[L^{71}R] do not surpass those for K1$_{HPg}$ and K4$_{HPg}$. Additionally, the K_d of t-AMCHA for r-K5$_{HPg}$[L^{71}R] is positioned between those for K1$_{HPg}$ and K4$_{HPg}$. These data suggest that the binding pocket of r-K5$_{HPg}$[L^{71}R] prefers ligands with more hydrophobic character between the amino and carboxylate groups of the ligand. Last, as evidenced by the lack of relevant fluorescence changes, binding of alkylamines likely did not occur with K5$_{HPg}$[L^{71}R]. Thus, it is clear that the presence of Leu^{71} in K5$_{HPg}$ plays a large role in the ability of these types of ligands to preferentially interact with K5$_{HPg}$. This is almost certainly due to the positioning of the Leu^{71} side chain in the binding pocket, which allows it to favorably interact with the terminal methyl group of straight-chain alkylamines.

In conclusion, it is clear from the above considerations that dramatic remodeling of the LBS of kringles is possible, an observation in concert with the fact that this pocket is preformed, as suggested here (Table 3), and shown in at least three other cases: those of K1$_{HPg}$ *(29)*, K4$_{HPg}$ *(30*, *41*, *58)*, and the Met^{66}Thr mutant of Lp(a)-K4−37 (unpublished results). That conformational rearrangements in kringles are not required to form the LBS simplifies its redesign. Such an accomplishment has been reported in other instances. In the case of K2$_{tPA}$, it has been shown that substitution of glutamic acid or glutamine for Lys^{33} at this same cationic locus allows strong binding of diaminohexane to this kringle *(49)*. Additionally, replacement of Tyr^{71} by tryptophan in K1$_{HPg}$ enhances binding of EACA to this polypeptide by an

order of magnitude *(24)*. The equivalent mutation, when engineered into wtr-$K5_{HPg}$, also resulted in an increase in the affinity of EACA, by approximately 3-fold *(26)*. Thus, it is evident that a tryptophan residue is preferred at this location in the binding pocket. From all of the foregoing data, we believe that it is possible to incorporate different ligand binding features into kringle domains, and to apply this information to the kringles of intact proteins. In this manner, it is possible to functionally isolate the contributions of individual kringles to protein function in multi-kringle proteins.

REFERENCES

1. McLean, J. W., Tomlinson, J. E., Kuang, W.-j., Eaton, D. L., Chen, E. Y., Gless, G. M., Scanu, A. M., and Lawn, R. M. (1987) *Nature (London) 330*, 132−137.
2. Marcovina, S. M., Hobbs, H. H., and Albers, J. J. (1996) *Clin. Chem. 42*, 436−439.
3. Kraft, H. G., Kochl, S., Menzel, H. J., Sandholzer, C., and Utermann, G. (1992) *Hum. Genet. 90*, 220−230.
4. Gunzler, W. A., Steffens, G. J., Otting, F., Kim, S. M. A., Frankus, E., and Flohe, L. (1982) *Hoppe-Seyler's Z. Physiol. Chem. 363*, 1155−1165.
5. Pennica, D., Holmes, W. E., Kohr, W. J., Harkins, R. N., Vehar, G. A., Ward, C. A., Bennett, W. F., Yelverton, E., Seeburg, P. H., Heyneker, H. L., Goeddel, D. V., and Collen, D. (1983) *Nature (London) 301*, 214−221.
6. Sottrup-Jensen, L., Claeys, H., Zajdel, M., Petersen, T. E., and Magnusson, S. (1978) *Prog. Chem. Fibrinol. Thromb. 3*, 191−209.
7. Lijnen, H. R., Hoylaerts, M., and Collen, D. (1980) *J. Biol. Chem. 255*, 10214−10222.
8. Lucas, M. A., Fretto, L. J., and McKee, P. A. (1983) *J. Biol. Chem. 258*, 4249−4256.
9. Clemmensen, I., Petersen, L. C., and Kluft, C. (1986) *Eur. J. Biochem. 156*, 327−333.
10. Hortin, G. L., Gibson, B. L., and Fok, K. F. (1988) *Biochem. Biophys. Res. Commun. 155*, 591−596.
11. Sugiyama, N., Sasaki, T., Iwamoto, M., and Abiko, Y. (1988) *Biochim. Biophys. Acta 952*, 1−7.
12. Thorsen, S., Clemmensen, J., Sottrup-Jensen, L., and Magnusson, S. (1981) *Biochim. Biophys. Acta 668*, 377−387.
13. Miles, L. A., and Plow, E. F. (1987) *Thromb. Haemostas. 58*, 936−942.
14. Ullberg, M., Kronvall, G., and Wiman, B. (1989) *APMIS 97*, 996−1002.
15. Wu, H. L., Wu, I. S., Fang, R. Y., Hau, J. S., Wu, D. H., Chang, B. I., Lin, T. M., and Shi, G. Y. (1992) *Biochem. Biophys. Res. Commun. 188*, 701−711.
16. Lind, S. E., and Smith, C. J. (1991) *J. Biol. Chem. 266*, 5273−5278.
17. Miles, L. A., Dahlberg, C. M., Plescia, J., Felez, J., Kato, K., and Plow, E. F. (1991) *Biochemistry 30*, 1682−1691.
18. Hortin, G. L., Trimpe, B. L., and Fok, K. F. (1989) *Thromb. Res. 54*, 621−632.
19. Miles, L. A., Fless, G. M., Scanu, A. M., Baynham, P., Sebald, M. T., Skocir, P., Curtiss, L. K., Levin, E. G., Hoover-Plow, J. L., and Plow, E. F. (1995) *Thromb. Haemostas. 73*, 458−465.
20. Christensen, U. (1985) *FEBS Lett. 182*, 43−46.
21. Tran-Thang, C., Kruithof, E. K. O., Atkinson, J., and Bachmann, F. (1986) *Eur. J. Biochem. 160*, 599−604.
22. Bajzar, L., Kalafatis, M., Simioni, P., and Tracy, P. B. (1996) *J. Biol. Chem. 271*, 22949−22952.
23. Lerch, P. G., Rickli, E. E., Lergier, W., and Gillessen, D. (1980) *Eur. J. Biochem. 107*, 7−13.
24. Menhart, N., Sehl, L. C., Kelley, R. F., and Castellino, F. J. (1991) *Biochemistry 30*, 1948−1957.
25. Sehl, L. C., and Castellino, F. J. (1990) *J. Biol. Chem. 265*, 5482−5486.
26. McCance, S. G., Menhart, N., and Castellino, F. J. (1994) *J. Biol. Chem. 269*, 32405−32410.
27. Novokhatny, V. V., Matsuka, Y. V., and Kudinov, S. A. (1989) *Thromb. Res. 53*, 243−252.
28. Marti, D., Schaller, J., Ochensberger, B., and Rickli, E. E. (1994) *Eur. J. Biochem. 219*, 455−462.
29. Mathews, I. I., Vanderhoff-Hanaver, P., Castellino, F. J., and Tulinsky, A. (1996) *Biochemistry 35*, 2567−2576.
30. Wu, T.-P., Padmanabhan, K., Tulinsky, A., and Mulichak, A. M. (1991) *Biochemistry 30*, 10589−10594.
31. De Marco, A., Motta, A., Llinas, M., and Laursen, R. A. (1986) *Arch. Biochem. Biophys. 244*, 727−741.
32. Thewes, T., Constantine, K., Byeon, I.-J. L., and Llinas, M. (1990) *J. Biol. Chem. 265*, 3906−3915.
33. Rejante, M. R., and Llinas, M. (1994) *Eur. J. Biochem. 221*, 927−937.
34. Varadi, A., and Patthy, L. (1981) *Biochem. Biophys. Res. Commun. 103*, 97−102.
35. Whitefleet-Smith, J., Rosen, E., McLinden, J., Ploplis, V. A., Fraser, M. J., Tomlinson, J. E., McLean, J. W., and Castellino, F. J. (1989) *Arch. Biochem. Biophys. 271*, 390−399.
36. Nilsen, S. L., DeFord, M. E., Prorok, M., Chibber, B. A. K., Bretthauer, R. K., and Castellino, F. J. (1997) *Biotech. Appl. Biochem. 25*, 63−74.
37. Chang, Y., Zajicek, J., and Castellino, F. J. (1997) *Biochemistry 36*, 7652−7663.
38. Tulinsky, A., Park, C. H., and Skrzypczak-Jankun, E. (1988) *J. Mol. Biol. 202*, 885−901.
39. Mulichak, A. M., Park, C. H., Tulinsky, A., Petros, A. M., and Llinas, M. (1989) *J. Biol. Chem. 264*, 1922−1923.
40. de Vos, A. M., Ultsch, M. H., Kelley, R. F., Padmanbhan, K., Tulinsky, A., Westbrook, M. L., and Kossiakoff, A. A. (1991) *Biochemistry 31*, 270−279.
41. Mulichak, A. M., Tulinsky, A., and Ravichandran, K. G. (1991) *Biochemistry 30*, 10576−10588.
42. Higashi, T. (1990) *J. Appl. Crystallogr. 23*, 253−257.
43. Wu, T.-P., Padmanabhan, K. P., and Tulinsky, A. (1994) *Blood Coagul. Fibrinol 5*, 157−166.
44. Navaza, J. (1994) *Acta Crystallogr. A50*, 157−163.
45. Brunger, A. T., Milburn, M. V., Tong, L., deVos, A. M., Jancarik, J., Yamaizumi, Z., Nishimura, S., Ohtsuka, E., and Kim, S. H. (1990) *Proc. Natl. Acad. Sci. U.S.A. 87*, 4849−4853.
46. Hendrickson, W. A. (1985) *Methods Enzymol. 115*, 252−270.
47. Finzel, B. C. (1987) *J. Appl. Crystallogr. 20*, 53−55.
48. De Serrano, V. S., and Castellino, F. J. (1992) *Biochemistry 31*, 3326−3335.
49. De Serrano, V. S., and Castellino, F. J. (1992) *Biochemistry 31*, 11698−11706.
50. Chibber, B. A. K., Urano, S., and Castellino, F. J. (1990) *Int. J. Pept. Protein Res. 35*, 73−80.
51. Forsgren, M., Raden, B., Israelsson, M., Larsson, K., and Heden, L.-O. (1987) *FEBS Lett. 213*, 254−260.
52. Castellino, F. J., Ploplis, V. A., Powell, J. R., and Strickland, D. K. (1981) *J. Biol. Chem. 256*, 4778−4782.
53. Mangel, W. F., Lin, B., and Ramakrishnan, V. (1990) *Science 248*, 69−73.
54. Ramakrishnan, V., Patthy, L., and Mangel, W. F. (1991) *Biochemistry 30*, 3963−3969.
55. Padmanabhan, K., Wu, T. P., Ravichandran, K. G., and Tulinsky, A. (1994) *Protein Sci. 3*, 898−910.
56. Arni, R. K., Padmanabhan, K., Padmanabhan, K. P., Wu, T. P., and Tulinsky, A. (1993) *Biochemistry 32*, 4727−4737.
57. De Serrano, V. S., Sehl, L. C., and Castellino, F. J. (1992) *Arch. Biochem. Biophys. 292*, 206−212.
58. Mulichak, A. M., and Tulinsky, A. (1990) *Blood Coagul. Fibrinol. 1*, 673−679.
59. Mikol, V., Lograsso, P. V., and Boettcher, B. R. (1996) *J. Mol. Biol. 256*, 751−761.
60. Atkinson, R. A., and Williams, R. J. P. (1990) *J. Mol. Biol. 212*, 541−552.

61. Byeon, I.-J., and Llinas, M. (1991) *J. Mol. Biol. 222*, 1035−1051.
62. Rejante, M. R., and Llinas, M. (1994) *Eur. J. Biochem. 221*, 939−949.
63. De Serrano, V. S., and Castellino, F. J. (1993) *Biochemistry 32*, 3540−3548.
64. Hoover, G. J., Menhart, N., Martin, A., Warder, S., and Castellino, F. J. (1993) *Biochemistry 32*, 1093610943.
65. Kelley, R. F., and Cleary, S. (1989) *Biochemistry 28*, 4047−4054.
66. De Serrano, V. S., and Castellino, F. J. (1994) *Biochemistry 33*, 3509−3514.
67. Laskowski, R. A., MacArthur, M. W., Moss, D. S., and Thornton, J. M. (1993) *J. Appl. Crystallogr. 26*, 283−291.

BI972284E